Pulsed current co-electrodeposition of kesterite Cu2ZnSnS4 absorber material on fluorinated tin oxide (FTO) glass under galvanostatic conditions

Patamaporn Termsaithong, Ratiporn Munprom, Akeel Shah, Aphichart Rodchanarowan

PII: S0257-8972(18)30406-7
DOI: doi:10.1016/j.surfcoat.2018.04.045
Reference: SCT 23329

To appear in: *Surface & Coatings Technology*

Received date: 16 November 2017
Revised date: 24 March 2018
Accepted date: 10 April 2018

Please cite this article as: Patamaporn Termsaithong, Ratiporn Munprom, Akeel Shah, Aphichart Rodchanarowan , Pulsed current co-electrodeposition of kesterite Cu2ZnSnS4 absorber material on fluorinated tin oxide (FTO) glass under galvanostatic conditions. The address for the corresponding author was captured as affiliation for all authors. Please check if appropriate. Sct(2017), doi:10.1016/j.surfcoat.2018.04.045

Pulsed Current Co-electrodeposition of Kesterite Cu_2ZnSnS_4 Absorber Material on Fluorinated Tin Oxide (FTO) Glass under Galvanostatic Conditions

Patamaporn Termsaithong[a], Ratiporn Munprom[a], Akeel Shah[b], Aphichart Rodchanarowan[a]*

[a]Department of Materials Engineering,Faculty of Engineering, Kasetsart University,

50 Ngamwongwan Rd., Ladyao, Chatuchak, Bangkok 10900, Thailand

[b]School of Engineering, University of Warwick, Coventry, CV4 7AL, UK

* Corresponding author: fengacrw@ku.ac.th

Abstract

The film of kesterite Cu_2ZnSnS_4 (CZTS) was prepared on a fluorinated tin oxide (FTO) substrate by a galvanostatically pulsed electrodeposition. The effect of duty cycles on electrodeposition was investigated at 33%, 50%, and 67% duty cycle. For the characterization, the prepared films were analyzed by scanning electron microscopy (SEM), energy dispersive spectroscopy (EDS), x-ray spectroscopy (XRD), UV-vis spectroscopy, Raman spectroscopy, and an atomic emission elemental analyzer. According to the experiments, surface morphologies of the CZT precursor appear to be uniform with fewer pores. After sulfurization, the morphologies of CZTS film become more uniform. When considering duty cycles, a higher duty cycle resulted in the surface being denser, more compact, more uniform, and smoother. Based upon the XRD and EDS, the film's composition consists of copper, zinc, tin, and sulfur. The compound formulae is also proved to be copper zinc tin sulfide.

Keywords: Kesterite; Cu_2ZnSnS_4 (CZTS); Duty cycle; Pulsed electrodeposition (PED); Galvanostatic conditions

1. Introduction

The world's population is projected to continuously increase. As our population increases the global energy consumption will increase in conjunction [1]. Solar energy is a promising candidate as a potential primary energy source in the future [2]. The harvesting of solar energy from sun light is of interest to a number of scientists and engineers because it is considered as one of efficient and clean energy conversion technologies, such as photovoltaic (PV) cells.

The use of PV cells has significantly grown for over decades [3-4]. This technology directly converts solar energy into electricity. Even though researchers have been intensively developing novel PV materials to improve efficiency, more than 80% of the current PV industry still heavily relies on the use of indirect band gap absorber materials, specifically single-crystal Si wafers. This material option provides high efficiency; however, it is still expensive [1-2, 5-6].

The recent PV developments have tended to focus on cost reduction using cheaper materials or more economical processing cost [7]. One of the major areas of development is thin film PV technologies, which are based on direct band gap materials such as copper indium (gallium) diselenide (CIGS), copper indium diselenide (CIS), and cadmium telluride (CdTe). These thin film PV developments have reached the commercial stage with the highest reported conversion efficiency about 36 % in module production [8-10].

Due to the high efficiency, thin film solar panels become a leading solar technology, and plus, they offer some advantages over monocrystalline Si technology, such as ease of installation. However, those thin films are still an issue since the commonly used materials such as Cd and Se are toxic, and In, Te, and Ga are scarce [11]. Hence, many researches are attempting to develop a PV technology based on non-toxic and abundant materials. Among all developments, a band gap p-type quaternary chalcogenide of copper zinc tin sulfide, Cu_2ZnSnS_4 (CZTS), has been a great candidate since it is non-toxic, easily available, and low cost.

Many studies reported several approaches to synthesize CZTS thin films including chemical and physical processes [12-14]. Due to many advantages of the chemical processes (non-vacuum) over the physical processes (vacuum)such as simplicity, scalability, cost effectiveness, low-temperature deposition capacity, and manufacturability, electrodeposition has been widely used to prepare photovoltaic CZTS thin films [15-20]. The used electrodeposition techniques include (i) sequential electrodeposition of metallic stacked thin layers on copper (Cu), zinc (Zn), and tin (Sn) followed by sulfur (S) diffusion, (ii) simultaneous electrodeposition of metallic Cu, Zn, and Sn thin film followed by S diffusion and (iii) single step electrodeposition of CZTS thin film followed by S diffusion [21-23]. Most of the abovementioned reports concentrate heavily on the electrodeposition of CZTS thin film on the molybdenum (Mo) as a back contact substrate. However, the price of Mo is high so it results in an increased expense in the sputtered Mo coated glass substrate [2]. Thus, an alternative of Mo back contract substrate is of great interest for CZTS thin film development.

As suggested by Nakada, the performance of semi-transparent CIGS using fluorinated tin oxide (FTO, SnO_2/F) as a back contact substrate is comparable to that of using Mo as a back contract substrate [24]. Moreover, Sarswat and Free also suggested that there was sufficient potential for electrochemically grown CZTS on FTO-coated glass as an alternative to CZTS on Mo-coated glass [2]. These reports in turn demonstrated that back contact alternatives such as FTO can be utilized for CZTS-based solar cell fabrication.

To fabricate CZTS-based solar cells, previous studies have employed direct current depositions under potentiostatic (voltage-controlled) and galvanostatic (current-controlled) conditions. Among all electrodeposition techniques, pulsed electrodeposition (PED) is frequently used to better control deposit properties. As mentioned by several studies, the PED offers advantages over conventional direct deposition techniques such as increasing deposition rate as

well as providing smooth surface morphology [24-28]. This technique applies a potential/current to a working electrode in a controlled fashion such as square wave, triangle wave, etc. and in turns provides smoother and finer electrodeposits [23-24, 29-31]. As shown in Fig. 1., there are at least three parameters including pulse height (current/potential amplitude (I_p or V_p)), relaxation time (T_{off}), and pulse time (T_{on}). Variation in these parameters can offer different deposit properties including uniformity and porosity.

Previously, Gurav *et al*. studied the implementation of pulsed electrodeposition (PED) to fabricate the CZTS thin film on a Mo back contact substrate under the potentiostatic condition [15]. However, PED has not yet been studied in the fabrication of CZTS thin film on FTO back contact materials under galvanostatic conditions. Therefore, in this study, we fabricate CZTS thin films under the galvanostatic condition by controlling I_p, T_{off}, and T_{on} and investigate the effect of on/off pulse time or a duty cycle of PED on deposit properties. The morphology, chemical composition, doping density and band gap energy of the electrodeposited CZTS films are discussed in this report.

2. Experimental

A two-electrode cell was used to perform the PED process under galvanostatic conditions. The counter electrode and working electrode are a platinum (Pt) electrode and a FTO-coated glass substrate, respectively. The dimension of the FTO-coated glass substrate exposed to electrolytes is approximately 1cm x1cm. The quantity of electrolytes used in all electrodeposition was 50 cm^3. All electrodeposition and electrochemical tests were conducted using Metrohm Autolab PGSTAT302N. The controlled current density (Ip) of 3 mA/cm^2 was used for all electrodeposition experiments. The effect of the duty cycle was studied by varying the amount of electrodeposition time. To control the total charge used for electrodeposition, the total amount of

electrodeposition time for 33% duty cycle, 50% duty cycle, and 67% duty cycle was 42.5 min, 28.05 min, and 21.25 min, respectively.

The electrolytic solution bath containing 0.004 M copper(II)sulfate pentahydrate ($CuSO_4.5H_2O$, Alpha Chemika), 0.15 M anhydrous zinc chloride ($ZnCl_2$, Alpha Chemika), 0.0180 M sodium stannate trihydrate ($Na_2SnO_3.3H_2O$, Carlo Erba), and 0.40 M potassium sodium tartrate tetrahydrate ($KNaC_4H_4O_6.4H_2O$, Fisher Chemical) as a complexing reagent was maintained at a constant temperature of 58 ^oC for the duration of electrodeposition. All chemicals had no further purifications. The as-deposited films were rinsed thoroughly with deionized water (Milli Q-type I ultrapure water: Millipore) and dried with argon gas.

The prepared film precursors were then subjected to sulfurization for 2 h in the argon environment with evaporated elemental sulfur in the annealing alumina tube furnace in order to reduce loss of conductivity. Prior to the sulfurization, the tube was purged with Ar gas for 15 min to remove air. The elemental sulfur (99.9% purity, Daejung Chemical and Metal) was used as the sulfur source. It was placed in an alumina boat and maintained at a temperature of 200 ^oC.

The films were characterized by scanning electron microscopy (SEM: Philips:XL30), x-ray diffraction (XRD; Philips:X'PERT), Raman spectroscopy (NT-MDT:NTEGRASpectra), UV-visiblespectroscopy (UV-vis 1700, Shimadzu), atomic emission elemental analyzer (liquid electrode plasma:LEP MH5000, Micro-Emission), Electrochemical impedance spectroscopy (MetrohmAutolab). For the Mott Schottky analysis carried out by a Metrohm Autolab PGSTAT302N potentiostat, the CZTS electrodes were immersed in aqueous solution of 0.07 M $Eu(NO_3)_3.6H_2O$, together with a saturated calomel reference electrode for measurements.

3. Results and Discussion

Before the sulfurization, the chemical composition of the co-electrodeposited films using different duty cycles was examined by Energy-dispersive spectroscopy (EDS), the results showed

that the films possessed an approximate Cu:Zn:Sn ratio of 2:1:1, which was desired for stoichiometric CZTS formation. The chemical composition of the precursor films was shown in Table 1. The co-electrodeposited films after the sulfurization were also examined using the same characterization technique. It was found that the films with an approximate stoichiometric Cu:Zn:Sn:S ratio of 2:1:1:4 were formed as shown in Table 2.

Fig. 2 a), b, and c) shows the XRD patterns of CZTS films grown on a FTO substrate at 67%, 50% and 33% duty cycle, respectively. Fig.2 a), b), and c) correspond to the reported kesterite structure of CZTS (JCPDS 26-0575), which exhibits four characteristic peaks of (112), (200), (220), and (312) at the 2θ values of 28.5^{o}, 33.0^{o}, 47.5^{o}, and 56.2^{o}, respectively. The average crystallite size of the coatings was also calculated from the full width at the half maximum (FWHM) of the peak using the Debye-Scherrer equation. Based on the XRD results, the crystallite size of films obtaining from pulsed current electrodeposition at 67%, 50%, and 33% duty cycles were 32.6, 35.4 and 39.2 nm, respectively. Based upon the above findings, it was found that increasing the duty cycles resulted in the slight decreasing the crystallite sizes, which is in good agreement with the SEM results.

However, in order to confirm that the observed XRD patterns belong to the CZTS film and not form other similar phases such as ZnS and Cu_2SnS_3 (CTS), the additional characterization was performed using Raman spectroscopy. Fig. 3 a), b), and c) show the Raman spectra of the electrodeposited CZTS films over the range of 275 to 400cm^{-1} at 67%, 50%, and 33% duty cycles, respectively. The major peaks at the approximate Raman shifts of 285 cm^{-1}, 337 cm^{-1}, and 370 cm^{-1} correspond to the CZTS film for all duty cycles, which was reported elsewhere [34-36]. In addition, there is a tiny distinct peak at 310 cm^{-1} and 470 cm^{-1} corresponding to CTS and CuS are observed, respectively. There is a lack of peaks or shoulders at 295 cm^{-1}, 348cm^{-1}, 351 cm^{-1}, and 355 cm^{-1}which contributes to the copper zinc tin (pulsed co-electrodeposited CZT) [35].

Film morphology of the pulsed co-electrodeposited CZT precursors and sulfurized CZTS films was analyzed and compared using SEM. The SEM images of the pulsed co-electrodeposited CZT precursors before sulfurization or sulfur diffusion under 67%, 50%, and 33% duty cycle of the galvanostatic electrodeposition at 3 mA/cm^2 are shown in Fig. 4 a), 4 c) and 4e), respectively. As observed by the SEM images, the CZT films deposited under various duty cycles possessed different morphology. The pulsed co-electrodeposited CZT films obtained at 33% duty cycle contained the large granules agglomerated from small grains which resulted in less compact, less uniform and higher porous film, while the pulsed co-electrodeposited CZT films obtained at the 50% duty cycle consisted smaller granules resulting in a film with higher compaction. Additionally, the pulsed co-electrodeposited CZT films obtained at 67% duty cycle appears to be uniform and contained voids at the surface. The SEM images of CZTS films after sulfurization obtained at 67%, 50%, and 33% duty cycle are demonstrated in Fig.2 b), d), and f), respectively. Among all films after sulfur diffusion, the CZTS film deposited at 33% duty cycle was least compact with surface voids due to the fusion of the grains [15,31]. This might be due to the fact that both CZTS and CTS phases were mixed in the film. In addition, the CZTS films deposited at 50% duty cycle was found to be more porosity as well as less uniformity than that deposited at 67% duty cycle. For the same duty cycle, the cross-sectional SEM images reveal the sulfurized CZTS films has more or less the same thickness as the co-electrodeposited CZT films. In addition, the sulfurized CZTS films is more compact than that of the co-electrodeposited CZT films.

The plot of transmittance versus wavelength for CZTS films at 67%, 50%, and 33% duty cycle is shown in Fig.5 a), b) and c), respectively. The CZTS films obtained from each duty cycle have shown the same transmittance behavior over the wavelength width. The transmittance profile of each sample generally shows the same trend, especially the visible light region.

However, some slight variations of transmittance profile were observed after the wavelength of 800 nm. This might be due to the nature of the film such as homogeneity and surface morphology [37-38].

Fig. 6 a), b) and c) show the plot of $(\alpha h\nu)^2$ versus photon energy ($h\nu$ of the sulfurized CZTS films deposited at 67%, 50%, and 33% duty cycle, respectively. By extrapolating the slope of the plot, the band gap energy can be obtained. As a result, the band gap energy values of the CZTS films obtained at 67%, 50%, and 33% duty cycles were 1.54, 1.52 and 1.48 eV, respectively. These reported values of band gap energy are consistent with values reported in other literature [5, 9-14, 36].

The doping density of the CZTS absorber layers was determined by measuring the apparent capacitance density as a function of potential, based on the Mott Schottky relationship below [31]:

$$\frac{1}{C_{sc}^2} = \frac{2}{e\varepsilon\varepsilon_0 N}\left[E - E_{FB} - \frac{k_b T}{e}\right]$$

Where C_{SC} is a capacitance of the space-charge region, e is an electronic charge, ε is the dielectric constant (10 for CZTS) [34], ε_0 is the permittivity of free space, N is a donor density (hole acceptor concentration for p-type semiconductor, E is the applied potential, E_{FB} is a flat band potential, k_b is Boltzmann's constant and T is temperature in Kelvin. Fig. 7illustrates Mott-Schottky plots (1/ C_{sc}^2 versus E) of the CZTS films grown on the FTO-coated substrate at 33%, 50%, and 67% duty cycle. The slope of the plot can determine the seminconducting type of films. Specifically, a positive slope indicates an n-type semiconducting film, while a negative slope exhibits a p-type semiconducting film. According to Fig. 7, a negative slope has been observed for all duty cycles. The results further confirmed the p-type semiconductor of the CZTS

films, which was in good agreement with the cathodic photocurrent. The donor density can be estimated from the slope. The obtained values of the charge carrier concentration for 67% duty cycle, 50% duty cycle, and 33% duty cycle correspondingly are 2.56×10^{16}, 2.55×10^{16}, and 2.55×10^{16} cm^{-3} which closely reflect reported values in other studies [8, 34, 39-48]. In addition, by the extrapolation of $1/ C_{sc}^2 = 0$, the flat band potential values of the films deposited at different duty cycles can be determined. The results indicated that the films grown at 67% duty cycle, 50% duty cycle, and 33% duty cycle possessed the flat band potential of 0.73 V, 0.72 V and 0.73 V vs saturated calomel reference electrode, respectively [35, 41-42].

4. Conclusion

The CZTS films have been successfully prepared by using the PED method under galvanostatic conditions. The films deposited at 67% duty cycle, 50% duty cycle, and 33% duty cycle possessed CZTS phase with the properly stoichiometric composition and optimal band gap of 1.5 eV. The CZTS obtaining from 67% duty cycle is morphologically more compact than that of 50% duty cycle and 33% duty cycle. Thus, the CZTS films produced by this procedure is also suitable to be used as an absorber for CZTS-based high-performance solar cells.

Acknowledgements

The financial support for this project provided by Kasetsart University Research and Development Institute (KURDI) is gratefully acknowledged. Financial support by the funding agency does not constitute endorsement of the contents of this paper. The authors would also like to acknowledge the Center for Advanced Separation Technology. Assistances from Mr.Nuttawich Techawibultanachok, Mr.Nattasak Sukkasem, and Dr.Attasit Tubtimtae are appreciated it.

References

[1] M.P. Suryawanshi, G.L. Agawane, S.M. Bhosale, S.W.Shin, P.S. Patil, J.H. Kim, A.V. Molholkar, CZTS based thin film solar cells: a status review, Mater. Technol. 28 (2013) 98-109.

[2] P.K. Sarswat, M.L. Free, A comparative study of co-electrodeposited Cu_2ZnSnS_4 absorber material on fluorinated tin oxide and molybdenum substrates, J. Electron. Mater. 41 (2012) 2210-2015.

[3] S.U. Nanayakkara, K. Horowitz, A. Kanevce, M. Woodhouse, P. Basore, Evaluating the economic viability of CdTe/CIS and CIGS/CIS tandem photovoltaic modules, Prog. Photovolt: Res. Appl. 25 (2017) 271-279.

[4] M.A. Green, K. Emery, Y. Hishikawa, W. Warta, E.D. Dunlop, D.H. Levi, A.W.Y. Ho-Baillie, Solar cell efficiency tables (version 49), Prog. Photovolt. Res. Appl. 25 (2017) 3-13.

[5] D.B. Mitzi, M. Yuan, W. Liu, A.J. Kellock, S.J. Chey, V. Deline, A.G. Schrott, A high-efficiency solution-deposited thin-film photovoltaic device, Adv. Mater. 20 (2008) 3657-3662.

[6] W.A. Badawy, A review on solar cells from Si-single crystals to porous materials and quantum dots, J. Adv. Res. 6 (2015) 123-132.

[7] J. Du et al., Zn-Cu-In-Se quantum dot solar cells with a certified power conversion efficiency of 11.6%, J. Am. Chem. Soc. 138 (2016) 4201- 4209.

[8] D. Barkhouse, O. Gunawan, T. Gokmen, T.K. Todorov, D.B. Mitzi, Device characteristics of a 10.1% hydrazine-processed $Cu_2ZnSn(Se,S)_4$ solar cell, Prog. Photovolt: Res. Appl. 20 (2012) 6-11.

[9] T.K. Todorov, J. Tang, S. Bag, O. Gunawan, T. Gokmen, Y. Zhu, D.B. Mitzi, Beyond 11% efficiency: characteristics of state-of-the-Art $Cu_2ZnSn(S,Se)_4$ solar cells, Adv. Energy Mater. 3 (2013) 34-38.

[10] M.A. Green, K. Emery, Y. Hishikawa, W. Warta, E.D. Dunlop, Solar cell efficiency tables (version 45), Prog. Photovalt: Res. Appl. 23 (2015) 565-572.

[11] B. Maniscalco, A. Abbas, J.W. Bowers, P.M. Kaminski, K.Bass, G. West, J.M. Wall, The activation of thin film CdTe solar cells using alternative chlorine containing compounds, Thin Solid Films. 582 (2015) 115-119.

[12] X. Jiang, L.X. Shao, J. Zhang, D. Li, W. Xie, C.W. Zou, J.M. Chen, Preparation of Cu_2ZnSnS_4 thin films by sulfurization of metallic precursors evaporated with a single source, Surf. Coat. Technol. 228 (2013) S408-S411.

[13] D. Tang, Q. Wang, F. Liu, L. Zhao, Z. Han, K. Sun, Y. Lai, J. Li, Y. Liu, An alternative route towards low-cost Cu_2ZnSnS_4 thin film solar cells, Surf. Coat. Technol. 232 (2013) 53-59.

[14] D.K. Kaushik, T.N. Rao, A. Subrahmanyam, Studies on the disorder in DC magnetron sputtered Cu_2ZnSnS_4 (CZTS) thin films grown in sulfide plasma, Surf. Coat. Technol. 314 (2017) 85-91.

[15] K.V. Gurav, J.H. Yun, S.M. Pawar, S.W. Shin, M.P. Suryawanshi, Y.K. Kim, G.L. Agawane, P.S. Patil, J.H. Kim, Pulsed electrodeposited CZTS thin films: effect of duty cycle, Mater. Lett. 108 (2013) 316-319.

[16] Y. Kim, J. Jaegoo, S. Kim, W.S. Chae, Cyclic voltammetric and chronoamperometric deposition of CdS, Mater. Trans. 54 (2013) 1467-1472.

[17] S. Kim, Y. Kim, J. Jung, W.S. Chae, Photoassisted electrodeposition of a copper (I) oxide film, Maters Trans. 56 (2015) 377-380.

[18] D. Hodges et al., Earth abundant and nontoxic absorber material for low cost, thin film solar cells**,** 2015 IEEE Conference on Technologies for Sustainability (SusTech). (2015) 53-58.

[19] H.W. Tsai et al., Facile growth of Cu_2ZnSnS_4 thin-film by one-step pulsed hybrid electrophoretic and electroplating deposition, Scientific reports. 6 (2016) 19102.

[20] M. Farinella, R. Inguanta, T. Spanò, P. Livreri, S. Piazza, C. Sunseri, Electrochemical deposition of CZTS thin films on flexible substrate, Energy Procedia. 44 (2014) 105-110.

[21] J.J. Scragg, D.M. Berg, P.J. Dale, A 3.2% efficient kesterite device from electrodeposited stacked elemental layers, J. Electroanal. Chem. 646 (2010) 52-59.

[22] K.V. Gurav, S.M. Pawar, S.W. Shin, M.P. Suryawanshi, G.L. Agawane, P.S. Patil, J.H. Moon, J.H. Kim, Electrosynthesis of CZTS films by sulfurization of CZT precursor: Effect of soft annealing treatment, Appl. Surf. Sci. 283 (2013) 74-80.

[23] S.M. Pawar, B.S. Pawar, K.V. Gurav, D.W. Bae. S.H. Kwon, S.S. Kolekar, J.H. Kim, Fabrication of Cu_2ZnSnS_4 thin film solar cell using single step electrodeposition method, Jpn. J. Appl. Phys. 51 (2012) 10NC27-1-4.

[24] T. Nakada, Microstructural and diffusion properties of CIGS thin film solar cells fabricated using transparent conducting oxide back contacts, Thin Solid Films. 480 (2005) 419-425.

[25] M.L. Free, R. Bhide, A. Rodchanarowan, Improving the morphology of copper electrodeposits from halide media using additives and mass transport control, ECS Trans. 13 (2006) 13-23.

[26] M.L. Free, A. Rodchanarowan, N. Phadke, R. Bhide, Evaluation of the Effects of Additives, Pulsing, and Temperature on morphologies of copper electrodeposited from halide media, ECS Trans. 2 (2006) 335-343.

[27] A. Rodchanarowan, P.K. Sarswat, R. Bhide, M.L. Free, Production of copper from minerals through controlled and sustainable electrochemistry, Electrochim. Acta. 140 (2014) 447-456.

[28] P. Kamnerdkhag, M.L. Free, AkeelA. Shah, A. Rodchanarowan, The effects of duty cycles on pulsed current electrodeposition of Zn-Ni-Al_2O_3 composite on steel substrate: microstructures, hardness and corrosion resistance, Int. J. Hydrogen Energy. 42 (2017) 20783-20790.

[29] M.I. Khalil, R. Bernasconi, L. Magagnin, CZTS layers for solar cells by an electrodeposition-annealing route, Electrochim. Acta 145 (2014) 154-158.

[30] S. Mandati, B.V. Sarada, S.R. Dey, and S.V. Joshi, Pulsed electrodeposition of $CuInSe_2$ thin films with morphology for solar cell applications, J. Electrochem. Soc. 160 (2013) D173-D177.

[31] K.V. Gurav, Y.K. Kim, S.W. Shin, M.P. Suryawanshi, N.L. Tarwal, U.V. Ghorpade, S.M. Pawar, S.A. Vanalakar, I.Y. Kim, J.H. Yun, P.S. Patil, J.H. Kim, Pulsed electrodeposition of Cu_2ZnSnS_4 thin films: effect of pulse potentials, Appl. Surf. Sci. 334 (2015) 192-196.

[32] K.J. Bryden, J.Y. Ying, Pulsed electrodeposition of $CuInSe_2$ thin films onto Mo-glass substrates, J. Electrochem. Soc. 158 (2011) B557-B561.

[33] P.K. Sarswat, M.L. Free, Demonstration of a sol-gel synthesized bifacial CZTS photoelectrochemical cell, Phys. Status Solidi A. 208 (2011) 2861-2864.

[34] P.K. Sarswat, M. Snure, M.L. Free, A. Tiwari, CZTS thin films on transparent conducting electrodes by electrochemical technique, Thin Solid Films. 520 (2012) 1694-1697.

[35] P.K. Sarswat, M.L. Michael, A. Tiwari, A comparative study of co-electrodeposited Cu_2ZnSnS_4 absorber material on fluorinated tin oxide and molybdenum substrates, J. Electron. Mater. 41 (2012) 2210-2215.

[36] H. Araki, Y. Kubo, A. Mikaduki, K. Jimbo, W.S. Maw, H. Katagiri, M. Yamazaki, K. Oishi, A. Takeuchi, Preparation of Cu_2ZnSnS_4 thin films by sulfurizing electroplated precursors, Sol. Energy. Mater. Sol. Cells. 93 (2009) 996-999.

[37] A. Wei, Z. Yan, Y. Zhao, M. Zhuang, J. Lui, Solvothermal synthesis of Cu_2ZnSnS_4 nanocrystalline thin films for application of solar cells, Int. J. Hydrogen Energy. 40 (2015) 797-805.

[38] H. Suarez, J.M. Correa, S.D. Cruz, C.A. Otalora, M. Hurtado, G.Gordillo, Synthesis and study of properties of CZTS thin films grown using a novel solution-based chemical route, Proceedings of the IEEE-Photovoltaic Specialists Conference, 16-21 June 2013, 2585-2589.

[39] F. Cardon, W.P. Gomes, On the determination of the flat-band potential of a semiconductor in contact with a metal or an electrolyte from the mott-schottky plot, J. Phys. D, Appl Phys. 11 (1978) L63.

[40] S. Delbos, Këwhile thin films for photovoltaics: a review, EPJ Photovoltaica. 3 (2012) 35004.

[41] J.J. Scragg, P.J. Dale, L.M. Peter, G. Zoppi, I. Forbes, New routes to sustainable photovoltaics: evaluation of Cu_2ZnSnS_4 as an alternative absorber material, Phys. Status Solidi. B Basic Solid State Phys. 245 (2008) 1772-1778.

[42] J.J. Scragg, P.J. Dale, L.M. Peter, Towards sustainable materials for solar energy conversion: preparation and photoelectrochemical characterization of Cu_2ZnSnS_4, Electrochem. Commun. 10 (2008) 639-642.

[43] T. Todorov, O. Gunawan, S.J. Chey, T.G. de Monsabert, A. Prabhakar, D.B. Mitzi, Progress towards marketable earth-abundant chalcogenide solar cells, Thin Solid Films. 519 (2011) 7378-7381.

[44] Y.L. Zhou, W.H. Zhou, Y.F. Du, M. Li, S.X. Wu, Sphere-like kesterite Cu_2ZnSnS_4 nanoparticles synthesized by a facile solvothermal method, Mater. Lett. 65 (2011) 1535-1537.

[45] S.M. Camara, L. Wang, X. Zhang, Easy hydrothermal preparation of Cu_2ZnSnS_4 (CZTS) nanoparticles for solar cell application, Nanotechnology 24 (2013) 495401.

[46] M. Tsuyoshi, N. Satoshi, W. Takahiro, First principles calculations of defect formation in In-free photovoltaic semiconductors Cu_2ZnSnS_4 and $Cu_2ZnSnSe_4$, Jap. J. Appl. Phys. 50 (2011) 04DP07.

[47] C. Calderón, G. Gordillo, R. Becerr, P. Bartolo-Pérez, XPS analysis and characterization of thin films Cu_2ZnSnS_4 grown using a novel solution based route, Mater. Sci. Semicond. Process. 39 (2015) 492-498.

[48] A. Safdar, M. Islam, I. Ahmad, A. Akram, M. Mujahid, Y. Khalid, Y. Zhu, Quantum confinement and size effects in Cu_2ZnSnS_4 thin films produced using solution processed ultrafine nanoparticles, Mater. Sci. Semicond. Process. 41 (2016) 420-427.

5. Tables

Table 1. The chemical composition of the pulsed co-electrodeposited CZT films (before sulfur diffusion) at various duty cycles characterized by EDS.

Duty cycle (%)	Atomic percentage		
	Cu	Zn	Sn
33	54	26	20
50	50	25	25
67	52	26	22

Table 2. The chemical composition of CZTS (after sulfur diffusion) at various duty cycles characterized by EDS.

Duty cycle (%)	Atomic percentage			
	Cu	Zn	Sn	S
33	28	7	11	54
50	25	10	12	54
67	27	11	12	50

6. List of figure captions

Fig. 1. Typical pulse current/potential diagram in square-wave pattern

Fig. 2. XRD patterns of CZTS film grown on FTO substrate at various duty cycles; (a) 67% duty cycle, (b) 50% duty cycle, and (c) 33% duty cycle. The main peaks observed at the 2θ values of 28.5º, 33.0º, 47.5º, and 56.2º corresponded to the CZTS phase

Fig. 3. Raman spectra of the CZTS film grown on FTO substrate at various duty cycles; (a) 67% duty cycle, (b) 50% duty cycle, and (c) 33% duty cycle. The peaks at the approximate Raman shifts of 285 cm^{-1}, 337 cm^{-1}, and 370 cm^{-1} are attributed to the CZTS film

Fig. 4. SEM surface image of films on FTO substrate at various duty under galvanostatic conditions, (a) co-electrodeposited Cu-Zn-Sn at 67% duty cycle, (b) sulfurized CZTS film at 67% duty cycle (c) co-electrodeposited Cu-Zn-Sn at 50% duty cycle, (d) sulfurized CZTS film at 50% duty cycle, (e) co-electrodeposited Cu-Zn-Sn at 33% duty cycle, and (f) sulfurized CZTS film at 33% duty cycle

Fig. 5. A plot of transmittance versus wavelength of sulfurized CZTS films deposited at various duty cycles; (a) 67% duty cycle, (b) 50% duty cycle, and (c) 33% duty cycle.

Fig. 6. A plot of $(\alpha h\nu)^2$ versus photon energy ($h\nu$ of the sulfurized CZTS films deposited at various duty cycles; (a) 67% duty cycle, (b) 50% duty cycle, and (c) 33% duty cycle.

Fig. 7 Mott-Schottky plot for CZTS film grown on coated-FTO at different duty cycles; (a) 67% duty cycles, (b) 50% duty cycle, and (c) 33% duty cycle

7. Figures

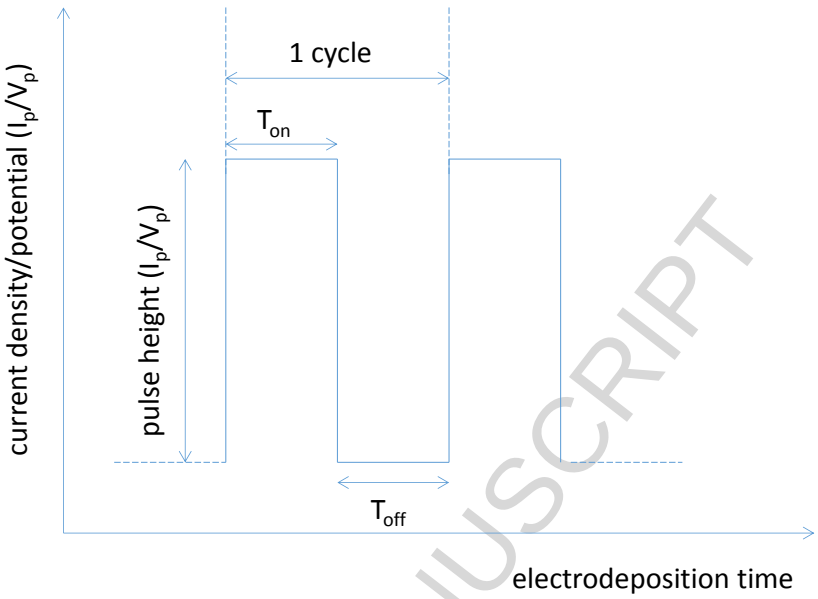

Fig. 1

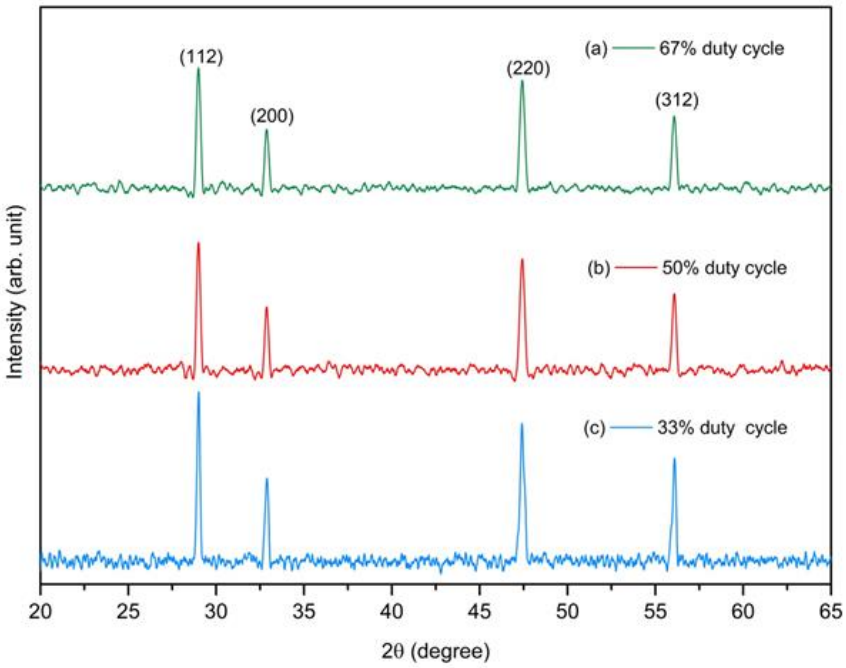

Fig. 2

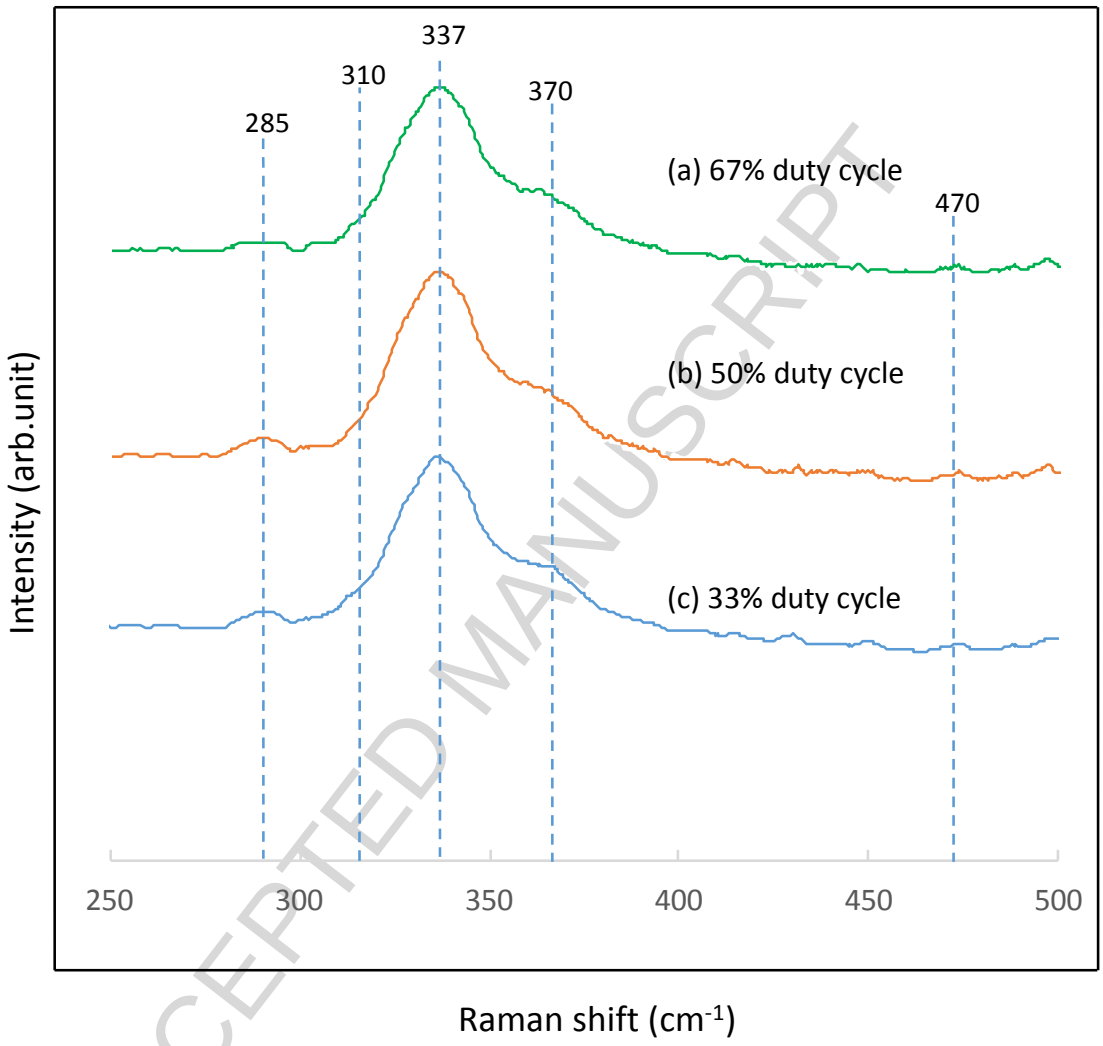

Fig. 3

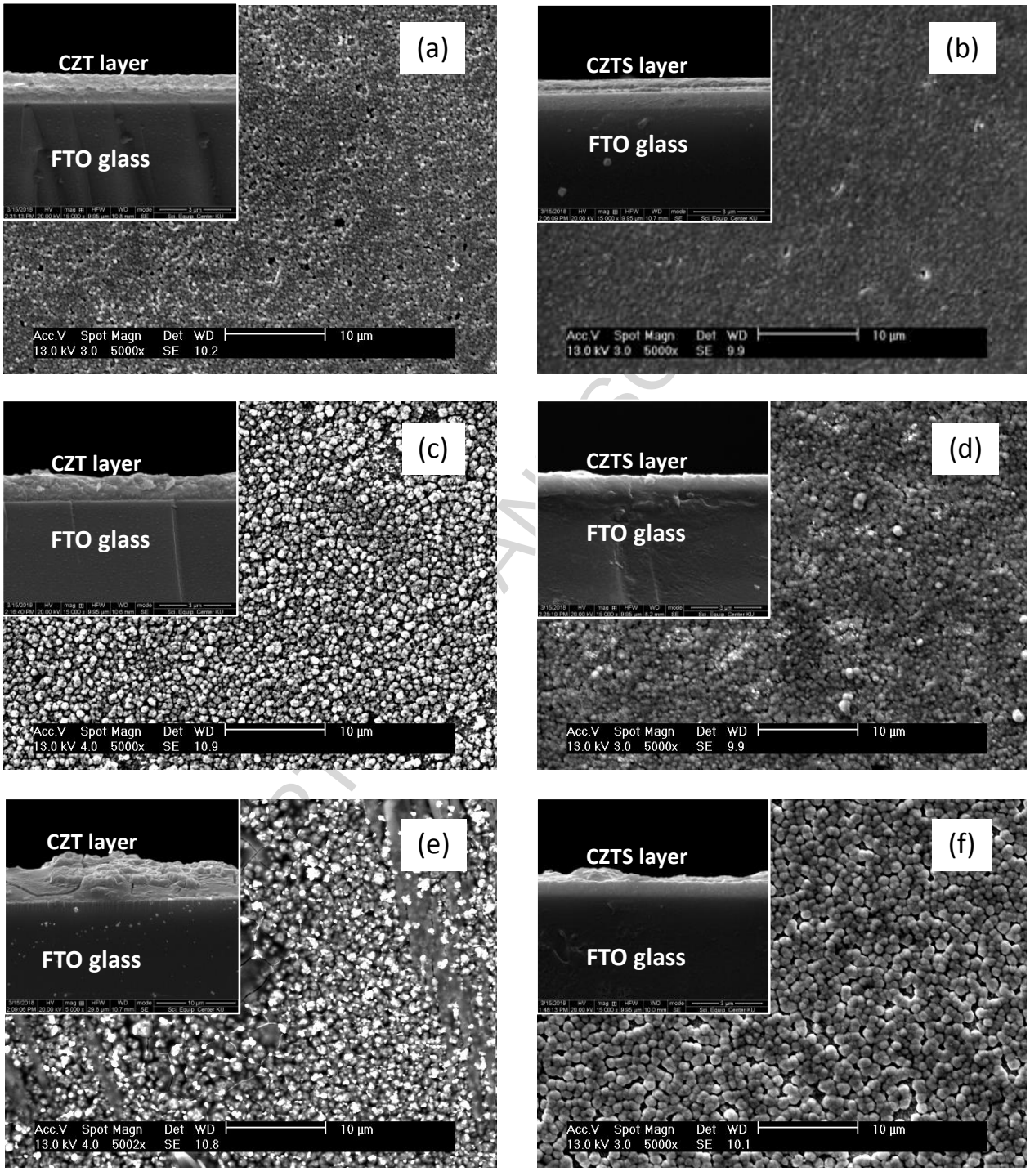

Fig. 4

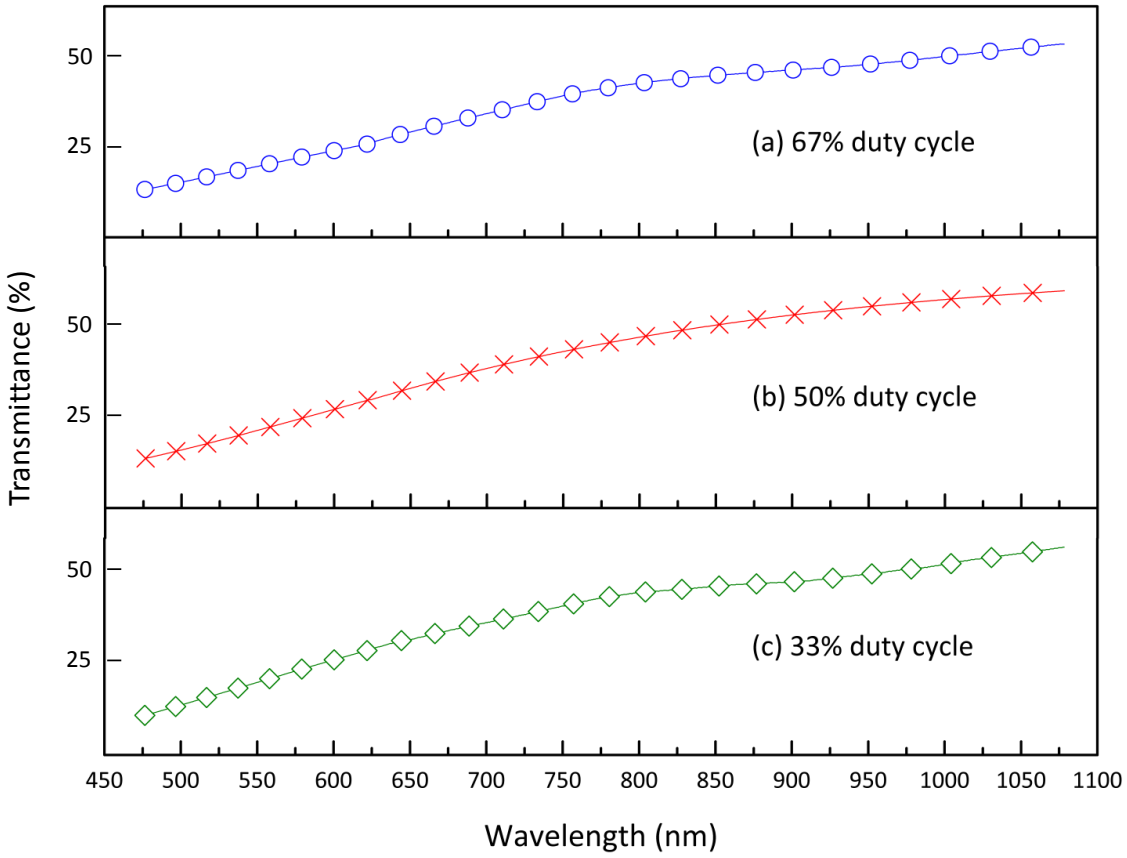

Fig. 5

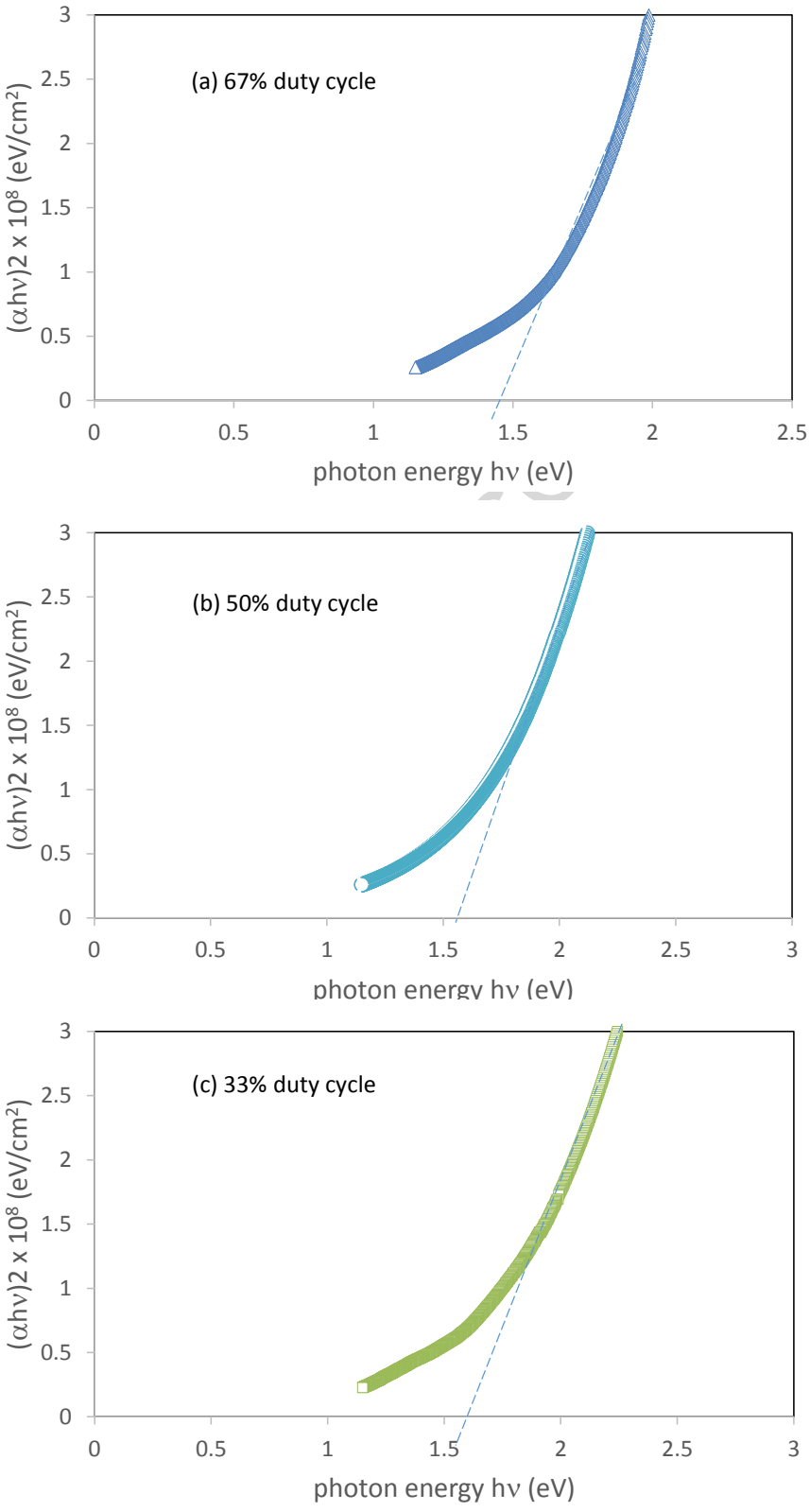

Fig. 6

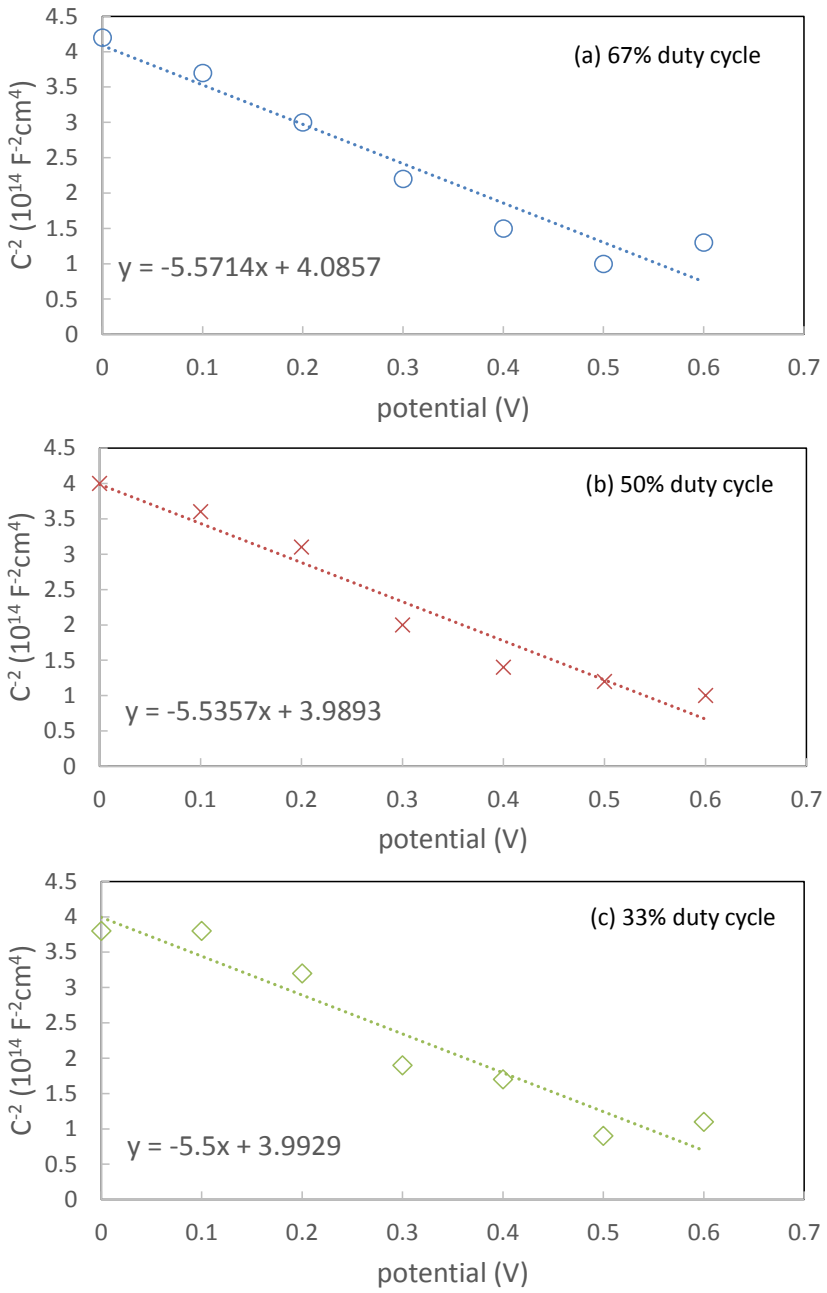

Fig. 7

Graphical abstract

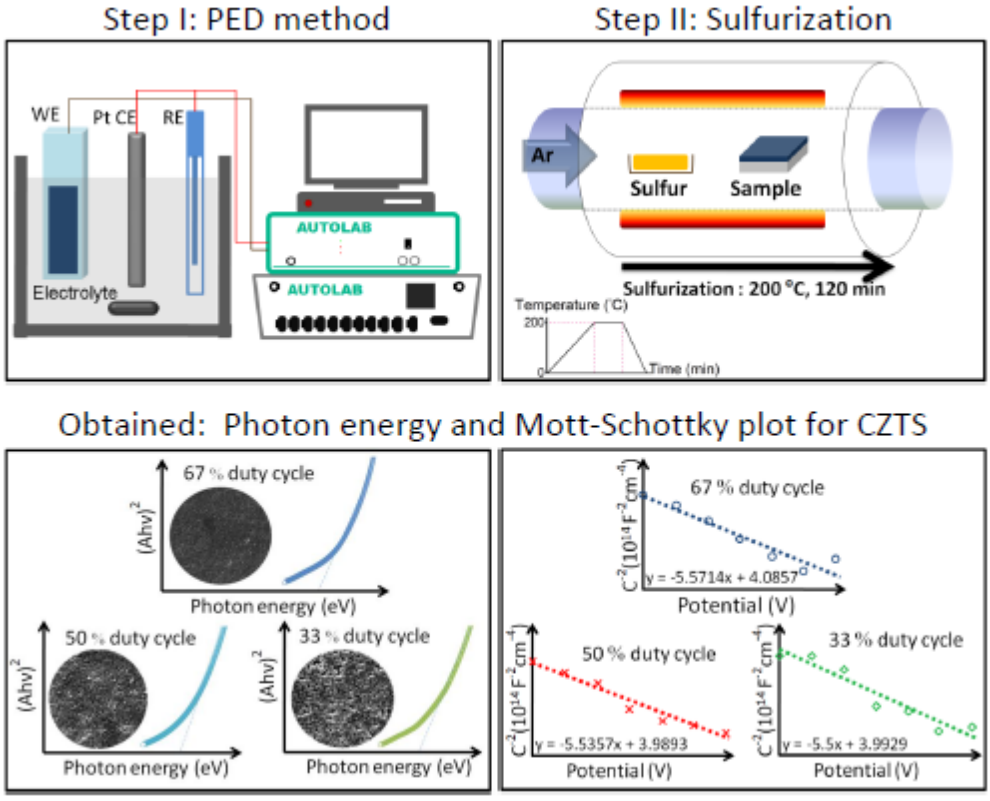

Highlights

- ✓ The CZTS thin films were successfully prepared by a gavanostatic PED method.
- ✓ The obtained CZTS films exhibit CZTS phase with proper stoichiometric compositions.with compact morphology.
- ✓ The CZTS films had a suitable band gap to be used as an absorber for solar cells.